*Biochimica et Biophysica Acta*, 986 (1989) 47–60
Elsevier



BBAMEM 74601

# Location and dynamics of alamethicin in unilamellar vesicles and thylakoids as model systems. A spin label study

Bernd Wille [1,*], Brigitte Franz [2] and Günther Jung [2]

[1] *Institut für Chemische Pflanzenphysiologie, and* [2] *Institut für Organische Chemie, Universität Tübingen, Tübingen (F.R.G.)*

(Received 20 February 1989)
(Revised manuscript received 18 July 1989)

Key words: Alamethicin; Spin label; Voltage-dependent channel; Membrane–peptide interaction; Thylakoid; ESR

**Location and dynamics of the voltage-dependent pore-forming icosapeptide alamethicin have been studied using spin labels which were linked directly and via spacers to the C-terminus of the amphiphilic α-helix. Ion-transport activities of these derivatives were found to be very similar to those of natural alamethicin in green plant thylakoids chosen as a model system. The shape of the electron spin resonance spectra indicates segmental motion of the nitroxide rather than rotation of the whole peptide. A population of spins showing narrow lines in the presence of thylakoids or lipid vesicles is attributed to alamethicin in the aqueous solution. A second population shows rotational correlation times greater than $10^{-9}$ s and is bound to the membranes, the C-termini residing in an environment with a polarity close to that of water. This population is inaccessible to the hydrophilic, charged line broadening agent chromium oxalate. Since spectral shapes and amplitudes of spectra are unchanged by additions of unlabelled peptide, it is concluded that the ESR detectable spins are bound to peptides essentially in the monomeric state. Alamethicin induced pore formation under flash illumination is demonstrated by measurement of kinetics of proton deposition in the thylakoid interior. When pores are opened by illuminating thylakoids and thus applying a membrane potential, mainly the bound population is affected by a process reversibly suppressing the signal, whereas only limited disappearance of label from the external medium is detected. Apparently, the potential causes a change in the conformation of the peptide which leads to a further immobilisation of the label, possibly due to a deeper insertion of the α-helices into the lipid membrane. However, evidence has been presented experimentally that there is no detectable change of potential prior to the opening of the pore.**

## Introduction

In 1968 it was established that alamethicin in planar lipid bilayers can induce voltage-dependent conductance and events closely ressembling action potentials [1]. The mechanism of pore formation of this polypeptide has attracted considerable interest [2]. Based on results from lipid bilayer experiments, the barrel stave model [3,4] had assumed alamethicin molecules lying on the membrane surface which would be flipped inside the membrane by an applied electric field to form ion-conducting pores by subsequent aggregation. It has been argued that most of the alamethicin molecules are oriented antiparallel inside the membrane if no potential is applied [5–8]. Extensive studies with chemically synthesized analogues have demonstrated that the minimum necessary structural element for channel formation is a simple α-helix spanning the membrane or at least in part its hydrophobic core [6,7].

Based on such evidence, the flip-flop gating model [5] has been proposed, which ascribes gating to a voltage-induced change of peptide helices from a preformed antiparallel aggregate to a parallel position, opening the channel by dipole–dipole repulsion. Each conducting

* Present address: Institut für Limnologie, Mayenbrook, D-2802 Ottersberg, F.R.G.

Abbreviations: 9AA, 9-aminoacridine; Aib, α-aminoisobutyric acid; Aca, 5-aminocaproic acid; ALA, alamethicin; Chl, chlorophyll; CP, 2,2,5,5-tetramethylpyrrolidine-1-oxyl-3-carboxylic acid; CrOx, potassium trisoxalatochromate(III); DCMU, 3′-(3,4-dichlorophenyl)-1′,1′-dimethylurea; DTA, 4-(dimethylamino)-2,2,6,6-tetramethylpiperidine-1-oxyl; FeCy, potassium hexacyanoferrate(III); Mes, 4-morpholineethanesulfonic acid; Tempamine, 4-amino-2,2,6,6-tetramethylpiperidine-1-oxyl; Tempone, 4-oxo-2,2,6,6-tetramethylpiperidine-1-oxyl; Tes, 2-{[2-hydroxy-1,1-bis(hydroxymethyl)ethyl]-amino}ethanesulphonic acid; Tricine, *N*-[2-hydroxy-1,1-bis(hydroxymethyl)ethyl]glycine.

Correspondence: G. Jung, Institut für Organische Chemie, Universität Tübingen, Auf der Morgenstelle 18, D-7400 Tübingen 1, F.R.G.

oligomeric pore would give rise to conductance levels resolvable in single-pore experiments by uptake and release of monomers. While this model describes nicely hysteresis phenomena of the channel conductance and ionic strength dependence of conductance levels, direct evidence for such a voltage-driven flop of helices is lacking to date. However, it has been shown that alamethicin induces lipid flip-flop in asymmetrical bilayers upon application of a voltage [9]. While this – as the author quoted did – may be attributed to structural disturbances or lipids passing the channel rather than lipids flipped together with alamethicin helices, it demonstrates that the event in question perturbs the membrane more than the mere lateral diffusion of helices would be assumed to do. Furthermore, the model has to assume a spontaneous flip-flop of some monomers to the *trans* side when alamethicin is added only to one side of the membrane to allow for the formation of antiparallel aggregates. Such a slow diffusion has indeed been detected [10].

Based on studies of the binding equilibrium of alamethicin to membranes and its kinetics at zero voltage, Schwarz attributed channel formation to a displacement of the binding equilibrium by an applied voltage, leading to increased concentration of peptide in the membrane and consequently to an aggregation [11].

While most arguments relevant to the discussion of such models could be derived from current voltage measurements, it seems that some salient features depend on information concerning the location of helices in or at the membrane and particularly their orientation during electrically silent steps of the gating mechanism. We have started to examine this by spin labelling the C-terminus of alamethicin and studying the ESR signals of these derivatives in two model systems:

- lipid vesicles for zero voltage experiments and
- chloroplast thylakoids for examination of the response to applied membrane potentials and ion gradients.

During the preparation of the manuscript, a study has been published which uses similar spin-label techniques and an ingenious labelling approach to probe the location of the peptide melittin in membranes of lipids vesicles [12].

## Materials and Methods

*Reagents.* Gramicidin D and valinomycin were obtained from Sigma, nigericin was from Eli Lilly, 9AA was from Serva, DCMU was recrystallized from chloroform and washed with light petroleum. CrOx was synthesized according to Ref. 13 and DTA by a modification of the method given in Ref. 14 for the secondary amine [15].

*Peptide analysis.* The peptides were checked for purity by thin-layer chromatography. $R_F$ values were determined using silica gel plates 60 $F_{254}$ (Merck, Darmstadt) at room temperature in solvent saturated glass chambers. The peptides were visualized by spraying with water and chlorine/4,4′-bis(dimethylamino)diphenylmethane (TDM). For HPLC chromatography we used a chromatographic system from Waters (conditions see Fig. 1, for preparative separations see below). Amino acid analyses were performed from total hydrolyzates (6 M HCl, 110 °C, 18 h) on a LKB amino acid analyzer. $^{13}$C-NMR spectra were recorded on the spectrometer WM 400 (Bruker-Physik, Karlsruhe) in [$^2$H]chloroform/methanol 1:1 or in [$^2$H]chloroform solution at 100.16 MHz and 25 °C.

*Synthesis of spin labeled alamethicin.* Due to the non-ribosomal biosynthesis of ALA [16] at least 12 components were detected by HPLC [17], and three main components were classified according to their $R_F$ (TLC) values as ALA F20, F30 and F50. ALA F50 posesses a glutaminyl residue in position 18, whereas ALA F30 has a glutamyl residue [18,19]. The N-terminus is blocked by acetyl-Aib [20] and the C-terminus consists of the amino alcohol, L-phenylalaninol [21,22]. In order to obtain chemically defined ALA labels we used only uniform ALA F50 preparations [23], which were selectively modified at the single functional group of the 20-peptide helix. Our ALA F50 preparations are only microheterogeneous with respect to Ala/Aib and Val/Aib exchanges. By comparison with highly pure synthetic alamethicin F30 [19] it has been demonstrated that analogues differing in these exchange positions do not exhibit remarkable differences in their pore-forming properties (Boheim, G. et al., unpublished data). Therefore the ESR signals of labelled corresponding analogues are not expected to exhibit detectable differences. ALA-CP was synthesized by direct esterification of the label with *N,N′*-dicyclohexylcarbodiimide and dimethylaminopyridine catalysis. For the introduction of spacer groups between ALA and CP we used *N*-benzyloxycarbonyl-ε-amino caproic acid (Z-Aca-OH) because the Z group can be removed from ALA-Aca-Z by mild hydrogenolysis to yield the amino acid ester ALA-Aca, whereas removal of the *tert*-butoxycarbonyl groups by trifluoroacetic acid may have led to partial hydrolysis of Aib-Pro peptide bonds in ALA [19]. The carboxy function of the ESR label CP was linked to the free amino group of ALA-Aca. The longest and polar spacer was introduced by coupling CP-$(Gly)_3$-OH to the amino acid ester ALA-Aca to give the label ALA-Aca-$(Gly)_3$-CP.

The labels ALA-CP and ALA-Aca-CP were purified by preparative HPLC using a chromatographic system of Waters: column 250 × 4.6 mm Lichrosorb C18, 10 μm; flow rate 1.3 and 1.8 ml/min; acetonitrile/water 85:15 isocratic; UV detection at 220 nm.

*Isolation and purification of alamethicin F50.* The mixture of natural alamethicin analogues was isolated

from the filtrate of a culture of the mycelium of *Trichoderma viride* NRRL 3199 according to Irmscher and Jung [23]. After acidification with HCl to pH 3, the filtrate was extracted with chloroform. After evaporation the extract was dissolved in methanol and the crude ALA was precipitated by addition of ether. After fractioning on Sephadex LH-20 in methanol, ALA positive fractions (TLC) were dissolved in 2-propanol and decolorized on charcoal Darco 60. Light petroleum (30–50 °C) was added to the filtered solution to precipitate alamethicin consisting of the three main components ALA F20, F30 and F50. Multiplicative countercurrent distribution in the system 2-butanol/0.05 M ammonium acetate (pH 8.7) (1 : 1, v/v) (300 transfers, 10 ml tubes; for details see also Ref. 24) was used to separate the main part of ALA F20 and F30. After 260 transfers ALA F50 was detected, which was further purified by chromatography on silicagel KG 60 (0.040-0.063 mm) from Merck (Darmstadt) using chloroform/methanol (2 : 1) as eluent. After a final gel chromatography on Sephadex LH-20, the component ALA F50 was pure according to TLC in the system chloroform/methanol/water (56 : 25 : 4) and HPLC revealed one main peak (Fig. 1). The isolated natural ALA F50 was characterized by $^{13}$C-NMR in methanol/chloroform 1 : 1 (Table I) and the chemical shift values were compared to those of highly uniform synthetic ALA F30 [25].

*Alamethicin [$^{20}$Pheol-2,2,5,5-tetramethylpyrrolidine-1-oxyl-3-carboxylate] (ALA-CP).* CP (9.3 mg, 50 μmol) from Aldrich was dissolved in the minimum amount of tetrahydrofurane and activated with 1 M dicyclohexylcarbodiimide/dichloromethane (20 μl) followed by addition of ALA (10 mg, 5 μmol) and dimethylaminopyridine (1.83 mg, 15 μmol). After 117 h the solvent was removed in vacuo and the crude ester ALA-CP was chromatographed on Sephadex LH-20 (column 37 × 2 cm; chloroform/methanol, 1 : 1). Yield 9.5 mg (87%). $R_F = 0.71$ (chloroform/methanol/acetic acid/water, 65 : 25 : 3 : 4); amino acid analysis corresponds to isolated Ala 1.7(2), Gly 0.8(1), Glx 2.9(3), Val 1.6(2), Leu 1.0(1), Aib n.d. Samples of ALA-CP were purified further by HPLC.

*N-Benzyloxycarbonyl-ε-aminocaproic acid (Z-Aca-OH).* ε-Aminocaproic acid (1 g, 7.6 mmol) in 2 M NaOH (3.8 ml; 7.6 mmol) was stirred at 0 °C. Benzylchloroformate (1.53 ml, 10.8 mmol) and 2 M NaOH (5.4 ml; 10.8 mmol) were dropwise added within 30 min. After 18 h 2 M HCl was added to precipitate Z-Aca-OH at pH 3–4. Z-Aca-OH was filtered off, dissolved in ethyl acetate and washed thrice with 5% potassium hydrogen sulfate and water, dried over sodium sulfate and precipitated with light petroleum. Yield 2.2 g (72%). $^{13}$C-NMR in chloroform: see Table I.

*Alamethicin [$^{20}$Pheol-6-benzyloxycarbonylamino hexanoate] (ALA-Aca-Z).* Z-Aca-OH (223 mg, 840 μmol) in dichloromethane was activated with *N,N'*-dicyclohexylcarbodiimide (840 μl of a 1 M solution in dichloromethane) and dimethylaminopyridine (102.6 mg, 840 μmol). After precipitation of dicyclohexyl urea a concentrated solution of ALA (84 mg, 42 μmol) in chloromethane was added. After 17 h at 45 °C, ALA was esterified and ALA-Aca-Z was isolated by gel chromatography on Sephadex LH-20 in chloroform/methanol (1 : 1). Yield 72.2 mg (81%). $R_F = 0.74$ (chloroform/methanol/acetic acid/water, 65 : 25 : 3 : 4); $R_F = 0.61$ (chloroform/methanol/water, 65 : 25 : 4); $R_F = 0.25$ (chloroform/methanol, 4 : 1). The product was characterized by amino acid analysis and in particular by $^{13}$C-NMR in chloroform solution which confirmed unequivocally its composition (see Table I). Samples were further purified by HPLC.

*Alamethicin [$^{20}$Pheol-6-aminohexanoate] (ALA-Aca).* A suspension of Pd/C in methanol was saturated with a constant stream of hydrogen and ALA-Aca-Z (23.3 mg; 10.5 μmol) in methanol was added. After 90 min the Z group was split off quantitatively (TLC) and ALA-Aca was isolated by gel chromatography on Sephadex LH-20 in chloroform/methanol (1 : 3) as a uniform (TLC) product. Yield 18 mg (93%). $R_F = 0.42$ (chloroform/methanol/water, 65 : 25 : 4); $R_F = 0.41$ (chloroform/

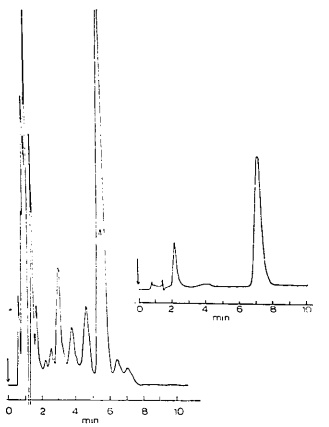


Fig. 1. HPLC chromatogram of natural microheterogeneous alamethicin after chromatography on silicagel and Sephadex LH-20. Conditions: Nucleosil C18, 5 μ; column: 250 × 4.6 mm; methanol/2-propanol/water (2 : 1 : 1) isocratic; flow rate 1.5 ml/min. Inset: rechromatography of the main component ALA F50 using a flow rate of 1.3 ml/min.

TABLE I

*$^{13}$C-NMR data on alamethicin F50 (ALA), the 6-aminohexanoate (ALA-Aca) and 6-benzyloxycarbonylamino-hexanoate of ALA (ALA-Aca-Z) and N-benzyloxycarbonyl-ε-aminocaproic acid (Z-Aca-OH) (100.1 MHz; c = 30 mg/ml; 25 °C)*

| Amino acid | ALA in $CD_3OD/CDCl_3$, 1:1 | ALA-Aca in $CD_3OD/CDCl_3$, 1:1 | ALA-Aca-Z in $CDCl_3$ |
|---|---|---|---|
| Gly $C_\alpha$ | 44.5 | 44.4 | 44.5 |
| Ala $C_\alpha$ | 52.7 48.4 | 52.6 48.8 | 52.5 49.0 |
| $C_\beta$ | 16.8(2×) | 16.8(2×) | 16.8(2×) |
| Val $C_\alpha$ | 64.3–63.6(2×) | 64.8–63.4(2×) | 66.4–63.2(2×) |
| $C_\beta$ | 29.8 29.5 | 30.8 29.6 | 29.7 29.3 |
| $C_\gamma$ | 20.2 19.9 19.3 19.0 | 20.3 19.9 19.3 19.1 | 20.4 19.9 19.2 19.0 |
| Leu $C_\alpha$ | 54.4 | 53.3 | 54.8 |
| $C_\beta$ | 40.7 | 40.1 | 40.4 |
| $C_\gamma$ | 24.9 | 24.9 | 24.6 |
| $C_\delta$ | 22.7 21.6 | 22.6 21.2 | 22.5 21.3 |
| Gln $C_\alpha$ | 57.2 53.4 53.0 | 56.5 52.9 52.8 | 56.8 53.1 52.8 |
| $C_\beta$ | 27.5 26.6 26.2 | 28.0 26.7 26.2 | 27.4 26.6 26.4 |
| $C_\gamma$ | 32.3(2×) 32.1 | 32.2 32.15 32.0 | 32.4 32.2 32.1 |
| Pro $C_\alpha$ | 64.3–63.6(2×) | 64.8–63.4(2×) | 66.4–63.2(2×) |
| $C_\beta$ | 29.3 29.1 | 29.6(2×) | 29.2 28.9 |
| $C_\gamma$ | 26.6 26.5 | 26.5(2×) | 26.5(2×) |
| $C_\delta$ | 49.5 49.1 | 49.5 49.3 | 49.7 49.3 |
| Aib $C_\alpha$ | 56.9 56.8(2×) 56.7 | 57.1(2×) 56.9 56.7(2×) | 56.8 56.6 56.5(2×) |
| | 56.6 56.6(2×) 56.5 | 56.6(2×) 56.4 | 56.4 56.3 56.2 |
| $C_\beta$ | 27.2 27.1(2×) 27.0 | 27.2 27.0(2×) 26.9(2×) | 27.2 27.0(2×) 26.9(2×) |
| | 26.9(2×) 26.3(2×) | 26.5 26.3(3×) | 26.2 26.1(2×) |
| | 23.7 23.4 23.1 | 23.6 23.3 23.1 | 23.8 23.3 23.0 |
| | 23.0 23.0 22.8(3×) | 23.0(2×) 22.8(3×) | 22.9 22.8(2×) 22.6(2×) |
| Phl $C_\alpha$ | 55.8 | 55.1 | 56.1 |
| Bzl $CH_2$ | 37.2 | 37.9 | 37.7 |
| $CH_2OH$ | 64.8 | 65.3 | 64.6 |
| aromatic | 138.7 129.6 128.4 126.4 | 137.7 129.5 128.6 126.8 | 137.9 128.5 127.9 126.3 |
| | C-1 C-3,5 C-2,6 C-4 | C-1 C-3,5 C-2,6 C-4 | C-1 C-3,5 C-2,6 C-4 |
| CO | 177.9 177.8 177.6 177.1 | 177.9 177.5 177.3 177.0 | 177.3 177.1 |
| | 176.8 176.6 176.6 176.3 176.0 | 176.7 176.6 176.5(2×) | 176.6(2×) 176.4(2×) 176.0 |
| | 175.9 175.8 175.2 175.1 | 175.9(2×) 175.0 | 175.6 175.4 175.2 175.0 |
| | 174.6 174.5 174.4 174.2 174.0 | 174.5(2×) 174.4(2×) 174.3(2×) 174.0(2×) | 174.5(2×) 174.2 174.19 174.0 |
| | 173.9 173.9 | 173.9(2×) 173.8 | 173.7 173.6(2×) 173.5 |
| | 172.9 171.6 171.3 | 172.6 171.6 171.3 | 172.8 171.9 170.9(2×) 170.8 |
| Z-CO | | | 156.6 |
| Ac-$CH_3$ | 22.4 | 22.4 | 22.5 |
| | Z-Aca-Gil in $CDCl_3$ | | |
| $C_\alpha C_\beta$ | 33.8 24.1 | 34.0 24.3 | 34.0 24.4 |
| $C_\gamma C_\delta$ | 25.9 29.3 | 25.7 29.3 | 26.0 29.2 |
| $C_\varepsilon$ | 40.9 | 40.6 | 40.9 |
| Bzl-$CH_2$ | 68.5 | | 66.4 |
| aromatic | 138.4 128.3 127.9 | | 136.9 129.4 128.3 128.0 |
| | | | C-1 C-3,5 C-2,6 C-4 |
| COOH | 178.7 | | |
| Z-CO | 158.5 | | 156.6 |

methanol/17% ammonia, 70 : 35 : 10); $R_F$ = 0.21 (chloroform/methanol/acetic acid/water, 80 : 20 : 3 : 4). $^{13}$C-NMR in methanol/chloroform 1 : 1: see Table I.

*Alamethicin [$^{20}$Pheol-6-(3-carbonyl-2,2,5,5-tetramethyl-pyrrolidine-1-oxyl)-aminohexanoate] (ALA-Aca-PC).* CP (1.2 mg, 6 μmol) in a minimal amount of dichloromethane was activated by *N,N'*-dicyclohexylcarbodiimide (20 μl of a 1 M solution in dichloromethane) and 1-hydroxybenzotriazole (0.8 mg, 6 μmol). ALA-Aca (2 mg, 1 μmol) and *N*-methylmorpholine (20 μmol) was added. After 10 h the solvent was removed in vacuo and the residue was chromatographed on Sephadex LH-20

in chloroform/methanol (1 : 1). Yield 1.7 mg (79%). $R_F = 0.58$ (chloroform/methanol/water, 65 : 25 : 4); $R_F = 0.69$ (chloroform/methanol/acetic acid/water, 65 : 25 : 3 : 4). Amino acid analysis found (calc.): Ala 1.97(2); Gly 0.89(1); Glu 3.13(3); Val 1.92(2), Leu 1.00(1), Pro 2.30(2), Aib n.d.

*N-(3-Carbonyl-2,2,5,5-tetramethylpyrrolidine-1-oxyl)-triglycine (CP-Gly$_3$-OH).* Preparation of CP-OSu: CP (13 mg, 69.8 μmol) and *N*-hydroxysuccinimide (HOSu; 10.4 mg, 90 μmol) in dichloromethane (300 μl) were esterified with *N,N'*-dicyclohexylcarbodiimide (90 μl of a 1 M solution in dichloromethane). The solvent was removed in vacuo, the residue dissolved in ethylacetate and the precipitated urea was filtered off. After evaporation of the solvent CP-OSu was obtained as an oily residue. Yield 14 mg (71%). $R_F = 0.83$ (chloroform/methanol/water, 65 : 25 : 4); $R_F = 0.75$ (chloroform/methanol/17% ammonia, 70 : 35 : 10).

Synthesis of CP-Gly$_3$-OH: H-Gly$_3$-OH (7.2 mg, 38 μmol) and sodium hydrogencarbonate (7.0 mg) were dissolved in warm ethanol/water (2 : 1). CP-OSu (5.4 mg, 19 μmol) in ethanol was added and the acylation followed by TLC. The solvent was removed in vacuo, the residue was dissolved in chloroform/methanol (1 : 1) and chromatographed on a silica gel column (particle size 60, 0.040–0.063 mm) to remove excess H-Gly$_3$-OH. Yield 4.9 mg (73%). $R_F = 0.21$ (chloroform/methanol/17% ammonia 70 : 35 : 10); $R_F = 0.06$ (chloroform/methanol/water, 65 : 25 : 4).

*Alamethicin [$^{20}$Pheol-Aca-Gly$_3$-CP] (ALA-Aca-Gly$_3$-CP).* CP-Gly$_3$-OH (2.1 mg, 5.8 μmol) in a small amount of dimethylformamide was activated by addition of 1-hydroxybenzotriazole (0.8 mg, 5.8 μmol) and 1 M *N,N'*-dicyclohexylcarbodiimide/dichloromethane (20 μl). After precipitation of urea ALA-Aca (3.4 mg, 1.64 mmol) in dimethylformamide was added. After completion of reaction (TLC) the solvent was removed in vacuo and the residue was chromatographed on Sephadex LH-20 in chloroform/methanol (1 : 1). UV-positive fractions (254 nm) were combined and lyophilized from *tert*-butanol. Yield 2.4 mg (63%). $R_F = 0.58$ (chloroform/methanol/17% ammonia, 70 : 35 : 10). Amino acid analysis found (calc.): Ala 2.0(2), Gly 3.6(4), Glu 3.1(3), Val 1.9(2), Leu 1.0(1).

*Stock solutions and lipids.* Ethanolic stock solutions of labels, unlabelled alamethicin and other ionophores were kept on ice or at −20 °C. The final concentration of ethanol in samples was kept below 2% if not otherwise stated. Soybean lipids were purchased from Sigma (phosphatidylcholine, commercial grade IIs). The product was ether-extracted [26], it contains about 19% phosphatidylcholine and mainly glycolipids [27]. Stock solutions were prepared in hexane and stored under nitrogen at −20 °C.

*Thylakoids.* Chloroplasts were prepared from lab-grown peas (14 days old seedlings), marked lettuce (outer mature leaves) or spinach according to [15] and osmotically broken in 5 mM $MgCl_2$. The material (referred to as thylakoids to emphasize the functional unit) was stored at a concentration of 4–8 mg/ml chlorophyll [28] in the dark on ice or 33% of volume ethyleneglycol were added and the preparation was frozen rapidly in small aliquots and stored under liquid nitrogen. All operations were carried out rapidly and as close to 0 °C as possible, resuspensions were done with a small brush. The resuspension buffer was 0.2 M sorbitol, 20 mM KCl, 5 mM $MgCl_2$, 0.2 mM Tes (pH 7.5).

*Lipid vesicles.* Vesicles were prepared in the resuspension buffer under omission of $MgCl_2$ and with 10 mM Tes according to Ref. 29 in an ultrasonic bath (small unilamellar vesicles, SUV) diameter as estimated by electron microscopy after contrasting with uranylacetate (16–250 nm) or by swelling into ion-free medium according to Ref. 30 (referred to as large unilamellar vesicles (LUV), diameter 30 nm to 4 μm). Lipid concentrations given in legends assume 100% yield of vesicle preparation.

*Fluorescence and oxygen evolution.* Oxygen evolution was detected polarographically in a thermostated Hansatec cuvette. The setup permitted simultaneous measurement of solution pH (Ingold Lot. 403-M3 chain) or of fluorescence. Fluorescence of 9AA was monitored with actinic light filtered with cut off filters of more than 600 and 670 nm and a Schott KG 3 heat filter. Excitation was delivered through a 404 nm interference filter (Balzers). Light sources were halogen lamps (Schott), intensities 1500 $W \cdot m^{-2}$ (actinic) and 4 $W \cdot m^{-2}$ (excitation). The photomultiplier (EMI 9558) was protected with a Balzers 461 nm interference filter and a Corning CS 4-96 filter. Some residual cross-talk of illumination was measured and corrected for. Measurements were done in the resuspension buffer mentioned, supplemented with 10 mM Tes, which kept the external pH constant within ±0.01 units. Correction for 9AA-binding in the light was done according to Ref. 31. Since addition of 1 mM $NH_4Cl$ to an alamethicin-decoupled sample caused no increase of fluorescence [32], binding was assumed to be proportional to the quench observed, i.e., to the pH-difference (which is a worst case assumption). The correction under this approximation is included in Fig. 2 (open circles). Since the correction is negligible for the values with low gradients used to calculate slopes it was omitted and the data displayed are uncorrected.

*Permeability.* We define a permeability of the thylakoid membrane for protons according to $J_H = P_H (h^l_i - h^l_e)$, the symbols denoting flux, permeability constant and proton concentration, respectively (subscripts; i, inner; e, outer volume; l, light; d, dark; H, protons). In the steady state, $h^l_i = \text{const}$, $J_{H,in} = J_{H,out}$ and $J_H$ is proportional to $r_{oxygen}$, the rate of electron transport as measured by oxygen evolution. We assume $(F_d/F_l - 1)$

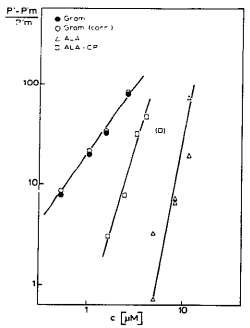


Fig. 2. Log/log-plot of permeability of thylakoid membrane induced by gramicidin D (Gram), alamethicin (ALA) and spin-labelled alamethicin (ALA-CP). Units of permeability of bare membrane, permeability without ionophore subtracted plotted against concentration of ionophore (added to aqueous volume); steady-state values at 14–15°C. 0.3 M sorbitol, 20 mM KCl, 5 mM $MgCl_2$, 10 mM Tes; electron acceptor 1.3 mM 2,6-dimethylquinone; 14°C, 28 μg/ml Chl, 13.3 μM 9AA (pH 7.45). ○, corrected for binding of 9AA in the light.

$= Q$ proportional to $\Delta h_i$ [33] for fluorescence measurements or $\Delta h_e$ proportional to $\Delta h_i$ for measurements of external acidification, the latter being a rather crude approximation since it is readily derived that $\Delta h_e = -V_i/V_e(h_i^l\beta_i^l/\beta_e - h_i^q\beta_i^q/\beta_e)$ ($\beta$ denotes the differential buffering capacity, $V$ volume), and it is well known that $\beta_i^l > \beta_i^q$ [34]. Thus $\Delta h_e < (-V_i\beta_i^{l,q}/V_e\beta_e)\Delta h_i$ and $\Delta h = h_i^l - h_e^l$, $h_e^l < h_e^q \leqslant h_i^q$; it follows $\Delta h_i < \Delta h$. We set $p' = r_{oxygen}/Q = C \cdot P_H$ [35]. It has been shown that ionophores do not change the buffering capacity of thylakoids in steady-state light [36]. If we assume now, according to Ref. 37, the aggregation of alamethicin to be completely cooperative and the concentration of monomers to be large compared to that of the aggregates, we find $\log(P_H - P_{Hm}) = \log K + n \log C_{ALA}$ ($P_{Hm}$: permeability of the bare membrane, $K$ association constant, $n$ molecularity of aggregation) or with the above definitions $\log[(p' - p'm)/p'm] = \log C' + n \cdot \log C_{ALA}$. The approximation in $p'$ if external alkalization is used in the measurements is expected to lead to an underestimation of the exponent.

*Electron spin resonance.* ESR measurements were taken using Varian E-line spectrometers at 100 or 25 kHz modulation and about 9.5 GHz. Samples were in glass capillaries (0.8 mm, supported by a 3 mm quartz tube for aqueous samples) or in flat cells in a Varian E 238 cavity with modified modulation coils. Temperature was approx. 23°C, unthermostated unless otherwise stated. Illuminations were provided by a halogen lamp (> 600 nm and heat filtered) through 100 × 1 cm light pipe or by a General Radio Strobotac with auxillary capacity (flash 8 μs at 1/3 height) through a lens (diameter 100 nm, $f = 30$ mm). A Bruker Aspect ER 140 Data system was used, field scans were calibrated using the large splitting of the galvinoxyl radical assumed to be 0.5961 mT [38].

Difference spectra were calculated introducing a variable factor which was set to one when this was expected (Fig. 3) or chosen empirically for an optimal baseline if unknown (Fig. 4). Sample volumes were 50 μl in capillaries, 200 μl in flat cells, for the exact conditions see legends to figures. Alamethicin was always added about 1 min after the whole sample had been pipetted.

Proton transport under flashing light was measured in the resuspension buffer in presence of chlorophyll (0.5 mg/ml), 10 to 20 mM CrOx and 0.6 to 3 mM DTA. The response time is 1 to 2 ms [15]. Computer fittings of kinetics were done using a nonlinear least-squares fit [39].

## Results

### *Action of alamethicin and spin-labelled derivatives on the thylakoid membrane*

The potential built up by thylakoids under illumination with single turnover flashes was estimated to be about 200 mV (inside positive) [40]; under continuous illumination it is about 80 mV, decreasing with increasing ionic strength [41]. A pH gradient will be built up of about 3 units in continuous light [33] and of about 0.05 unit after a single flash [42]. Electron transport and the proton gradient at the membrane are measured simultaneously. An extra permeability induced by ionophores will bring about an increase in the rate of electron transport and a reduction of the gradient. Assuming complete cooperativity of aggregation and an excess of monomers of alamethicin over the aggregates a log–log plot of added alamethicin concentration against this extra permeability will produce a straight line with a slope giving the number of monomers per conducting aggregate. In our system, however, ionophores will tend to collapse the voltage, and the assumption of complete cooperativity is unreasonable; so we are actually doing a bioassay allowing for a phenomenological comparison of ionophores and giving a lower limit of the molecularity. The process can be followed over a limited range of ionophore concentrations. Above it the apparent permeability collapses due to limitations in the detection of small gradients and possibly due to secondary effects of the peptides (bracketed point in Fig. 2).

Permeabilities were measured using the steady-state values rather than the decay after turning off the light, since the latter is known to be influenced by transient

TABLE II

*Apparent molecularities of the pore-forming reaction of alamethicin and spin-labelled derivatives*

Slopes obtained graphically from the steepest part of the functions (details see Materials and Methods). Least-squares analysis of all points produced $n > 5$ with alamethicin. Conditions: 13–28 μg/ml Chl pH 7.5–7.92, 14–15°C. Data from decoupling-experiments.

| Ionophore | Exponent | |
|---|---|---|
| Gramicidin D | 1.75 | ($n = 1$) |
| Alamethicin | 5.3 ±1.4 | ($n = 4$) |
| ALA-CP | 4.36±0.45 | ($n = 3$) |
| ALA-Aca-CP | 4.0 ±0.17 | ($n = 3$) |

diffusion potentials of counterions [43]. Fig. 2 shows typical results with different ionophores and one thylakoid preparation. Table II gives the data obtained at 14–15°C with different thylakoid preparations. A value of one for the exponent has been reported for gramicidin with a fluorescence technique at (presumably) room temperature and low osmolarity [35]. When external pH changes were used to obtain an estimate of the proton gradient, the exponents were lower (3.5 for ALA, $\leq 1$ for gramicidin), addition of 50 nmol of valinomycin per mg of chlorophyll did not change these values. The amounts of the derivatives needed to produce a permeability 10-fold that of the bare membrane were similar with a lot of scatter, and of the order of 100 nmol ALA-derivatives per mg chlorophyll. These particular experimental results (Fig. 2) were obtained with a crude preparation of unlabelled alamethicin, therefore higher concentrations were required than with the labelled pore formers. Since the polarity of the electric field of thylakoids is negative outside and alamethicin pores are believed to open only from the positively polarized side of a membrane, gating in this system requires the passage of some molecules over the membrane (see Discussion) [40]. We found this process must be very quick: if alamethicin was injected in the light, the time until the gradient began to decay was essentially the time required to mix the contents of the cuvette.

*Action of alamethicin on proton transport on a rapid time scale*

Proton transport by thylakoids after short flashes was followed using the distribution of DTA, broadening the signal of external amine with CrOx and taking kinetics on the low-field line of the internal signal [15]. The decay of the signal, which shows usually half-times of 15 to 30 s was found to be accelerated at concentrations of more than 100 nmol ALA per mg Chl and at lower concentrations for the ALA derivatives. This effect is most likely to be attributed to chaotropic actions of these compounds, since the channel conductance of alamethicin should discharge the small coupling units

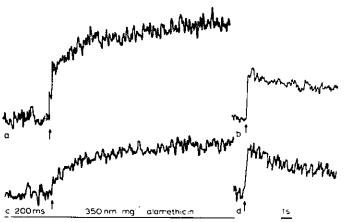


Fig. 3. Action of alamethicin on proton transport in thylakoids on a rapid time scale after short flashes. Thylakoids, 0.57 mg/ml Chl 0.3 M sorbitol, 17 mM KCl, 4.25 mM $MgCl_2$, 37.5 mM CrOx, 0.6 mM DTA, 0.266 mT, 100 mW; kinetic traces taken on positive low field peak of DTA-signal ($\tau$: amplifier time constant) (a) 100×, $\tau = 100$ μs, scan 200 ms, computer fit: 62% $t_{1/2} < 3$ ms, remainder $t_{1/2} \approx 32$ ms. (c) 200×, same conditions, 350 nmol/mg alamethicin computer fit: $t_{1/2} < 3$ ms: 24%, remainder $t_{1/2} \approx 15$ ms. (b) as (a) $\tau = 30$ ms scan 10 s; (d) as (c) $\tau = 30$ ms scan 10 s.

very rapidly. Indeed, the amplitude of the signal was reduced at lower concentrations. Fig. 3 shows the underlying effect: the initial rise of the signal is diminished in 3c compared to 3a, whereas the slow decay (3b vs. 3d) is scarcely affected. Since it is known that ionophores lead to the disappearance of rapid phases in proton liberation [44,46], it was checked with gramicidin that this effect was absent in the preparation used (lettuce chloroplasts (pH 7.4) 23.8 nmol gramicidin/mg Chl, flashes 1 Hz, no FeCy present), in accordance with a recent report [45].

*Spectra of alamethicin labels in organic solvents*

We calculated $\tau_c$ values from the spectra using the peak-ratio method and the formula given by Keith et al. [46]. The constant was assumed to be $6.5 \cdot 10^{-10}$ [47]. We did not apply more sophisticated approaches [48–50] here, since we usually have to face problems of unresolved contributions in the baseline. Small amounts of endogeneous thylakoid signals or small amounts of immobilized label (a general problem which caused us to be careful in interpreting the data in Table III) can be expected to distort results from most methods using fits severely. We are left with the approach of Kusnetsov et al. [51]: measurements were done in aerobic solvents, keeping the experimental linewidth well above 0.12 mT, where the natural linewidth will approach the apparent linewidth of the composite line. Table III shows some data from anaerobic samples as well to give an idea of the possible errors.

The motional parameters estimated apply to the nitroxide group. While it has been shown that labels attached to proteins sense conformational changes of the macromolecule [47], and namely those conjugated to

an α-helix may be immobilized [52], attachment to a random coil or to side-chains of a helix [47] may lead to motion considerably faster than that of the big molecule. Table III shows that the motion of CP is hindered by the attachment to alamethicin, and the more the shorter the spacer-group between Pheol and CP (see values obtained in dioxane). The spectra show slow variations in dichloromethane, dioxane and water at pH 7 (broadening of the signals and slow shifts in $\tau_c$), particularly with the ALA-CP. In pure hexane, this derivative (not the others) produced only broadened signals, which narrowed upon addition of ethanol. Mixing in unlabelled alamethicin made turn up the signal of an immobilized population indicating that mixed aggregates form under these conditions. The values given refer to samples 5–15 min after preparation and were constant during this time. Addition of high concentrations of unlabelled alamethicin to samples prepared in dioxane did not cause further immobilisation.

Since changes in rotational time with viscosity depend on the 3rd power of molecular radius, the similar change in $\tau_c$ when going from water to the viscous 1-octanol with CP and the labelled peptides implies that the label in our alamethicin derivatives indicates mainly segmental motion. The rather low hindrance in octanol (mainly monomeric alamethicin) and the rather high value in dioxane (mainly aggregates [21,53–55]) indicate that aggregation of peptide is still sensed as further hindrance in rotation.

*Spectra in vesicles and thylakoids*

The signals were essentially stable after the time required for sample preparation. They were not influenced by the potentials built up at the vesicle membrane due to additions such as CrOx or buffers, since addition of nigericin (5 μM) and valinomycin (10 μM) prior to alamethicin labels did not change the results. The most prominent feature of the results at 1–40 mg/ml soybean lipid and 0.2–1 mg/ml Chl with thylakoids is seen in the spectra of Figs. 4a, 5a and 6a (big lines in 5a only, see below): the increase of the relative amount of narrow signal with increasing length and hydrophilicity of the spacer is far more drastic than expected when elongating the label from an aggregate (see dioxane values in Table III).

The addition of CrOx broadens lines of nitroxides accessible to the trisoxalatochromate anion by Heisenberg exchange [56,57], leaving the spin signals inaccessible to the outer aqueous volume. Residual differences in the shapes of signals shown in Figs. 4b, 5b and 6b may be due to insufficient CrOx. Spectra in LUV and SUV were essentially identical for a given ALA derivative. LUV have been introduced to provide a larger internal volume and to facilitate detection of internal signals (see below).

The spectrum of ALA-$Gly_3$-CP in SUV can be resolved to a narrow and a broad component (Figs. 5b and c). The signal in the presence of CrOx (spectra from exterior of vesicles broadened) is corrected by subtract-

TABLE III

*Motion parameters for labelled alamethicin in organic solvents*

Modulation ⩽ 20 μT, microwaves ⩽ 5 mW. Thylakoids and vesicles: modulation below 1/3 linewidth, microwaves ⩽ 20 mW.

| Solvent | Rotational correlation times | | | | | | |
|---|---|---|---|---|---|---|---|
| | $\tau_c$ [$10^{-11}$ s] [a] | | | | | | $\frac{\tau_c\text{(ALA-Aca-CP)}}{\tau_c\text{(CP)}}$ |
| Label: | CP | | ALA-CP | ALA-Aca-CP | | ALA-$Gly_3$-Aca-CP | |
| | $+O_2$ | $-O_2$ | | $+O_2$ | $-O_2$ | | |
| $CH_2Cl_2$ | 3.5 | 9.8 | 15 | 17.4±1 | 17 ± 4 | – | 5.0 |
| Dioxane | 4.1 | 2.9 | 35.6 | 31.7±4 | 37.2± 3 | 27.5 | 7.7 |
| Octanol-1 | 41.5 | 28.0 | 166 | 119 ±7 | 134 ±12 | – | 2.9 |
| $H_2O$ (pH 9) | 3.6 | – | 43 | 19.2 | – | – | 5.3 |
| $H_2O$ (pH 7) | 3.5 | 4.7 | 28 | 19.3 | 17.2 | 14.8 | 5.6 |
| SUV [b] | | | | | | | |
| CrOx 40 mM | – | – | 350 | 109 | – | 69 | – |
| Thylakoids [b] | | | | | | | |
| +CrOx | – | – | 109 [c] | 120 [d] | – | 113 [e] | – |
| −CrOx | – | – | – | 25.2 | – | – | – |

[a] Theory valid only up to $10^{-9}$ s.
[b] Values depend on preparation used.
[c] 60 mM CrOx.
[d] 75 mM CrOx.
[e] 60 mM CrOx. Samples in organic solvents contain < 15 μM label and ⩽ 4% ethanol.

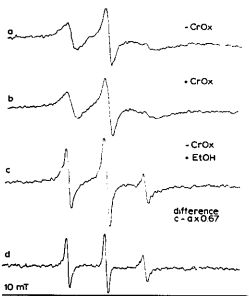


Fig. 4. ESR spectra of ALA-CP in large unilamellar vesicles (LUV), retraced. 40 mW, 106 μT (slightly overmodulated), 10 μM ALA-CP, ≈13.5 mg/ml soybean lipid, 54 mM CrOx if present, 90 mM Tricine (pH 7.5), 0.3 M sorbitol, 1.8 mM $MgCl_2$, 7.2 mM KCl. (a) No additions; (b) + CrOx; (c) 10% ethanol; (d) difference (c) − (a). factor optimized for clean baseline.

ing a spectrum without vesicles to eliminate residual broadened signal. The result (Fig. 5b) is the broad component. Subtracting this from Fig. 5a leaves the narrow one detectable only in the absence of CrOx. The $\tau_c$ obtained from the shape of Fig. 5b (or 4b and 6b) is higher than $10^{-9}$ s, the limit of validity of the theory [58] used to calculate it. The narrow spectra are very similar to the spectra in water. Examination of the wings of the lines clearly shows that the broad spectrum

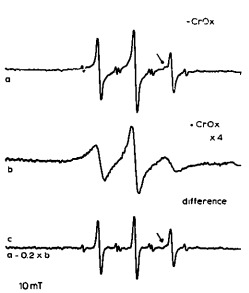


Fig. 5. ESR spectra of ALA-Aca-$Gly_3$-CP in small unilamellar vesicles (SUV). Peptide conc. 20 μM, SUV 1.9 mg/ml soybean lipid, spectra 2 min scan, $\tau = 64$ ms, 10 mW, 53 μT, 0.3 M sorbitol, 225 mM Tricine (pH 7.5), 20 mM KCl, 5 mM $MgCl_2$. (a) + 20 μM ALA-Aca-$Gly_3$-CP, + 250 mM KCl. (b) ALA-Aca-$Gly_3$-CP + 74 mM CrOx, corrected by subtracting blank without SUV. (c) Difference of spectra (a) − (b).

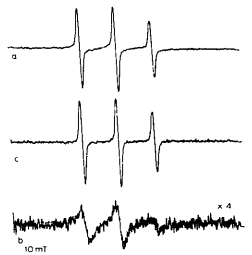


Fig. 6. ESR spectra of different spin-populations of ALA-Aca-CP in thylakoids. Thylakoids 0.57 mg/ml Chl, 16.7 nmol ALA-Aca-CP/mg Chl, 0.3 M sorbitol, 48 mM Tricine (pH 7.5), 1.6 mM FeCy, 250 mM KCl, 5 mM $MgCl_2$, 53 μT, 40 mW, scan 2 min, $\tau = 64$ ms, scans taken after several light/dark cycles, not corrected for signal I (see Fig. 7) which is negligible under these conditions. (a) + 120 mM KCl; (b) + 38 mm CrOx. Factor in difference optimized for clean baseline.

exists in the absence of line-broadening agent. The spectrum of ALA-CP (Fig. 4a) without CrOx shows a very small contribution of narrow signal (compare ALA-$Gly_3$-CP in a similar sample; Fig. 5a). The intermediate situation is realized with ALA-Aca-CP and thylakoids (vesicles produce comparable results). At high concentrations of alamethicin labels or at high ionic strength in thylakoids an extra signal turned up, consisting of two satellites to each nitroxide line, the groups showing a splitting due to an $I = 1$ nucleus of 1.46 mT and situated not exactly symmetrical to the proxyl lines, especially at the high-field line, where a shoulder indicates a central line in the additional signal (arrow). Hence we would interpret the second splitting as due to two protons or an $I = 1$ nucleus with $A = 0.393$ mT in either case. This signal was shown to exist also in the presence of an up to 15-fold excess of unlabelled peptide.

Areas of lines, i.e., relative amounts of spin populations were calculated using the approximation $A = p \cdot h \cdot \Delta W_{pp}^2$ (the symbols denoting area, a constant factor, first derivative line height, and peak to peak width, respectively) under the reasonable assumption of a constant line shape. The above subtraction procedure allows a limited resolution of the contributions of different populations to the spectra.

With soybean lipids the amount of broad signal varied from 6% at 14 μM to 78% at 57 mM lipid (assuming a molecular mass of 750 kDa) at 24 μM ALA-Aca-CP. At 46 mM lipid the broad component accounted for 81% with Ala-CP and 39% with Ala-Aca-$Gly_3$-CP. Preliminary experiments showed that, when chloroplasts were centrifuged down rapidly (2 min), the

amount of narrow signal in the supernatant was virtually equal to that in the sample whereas the broad component accumulated in the pellet. We can not rule out shifts in the binding equilibrium during centrifugation, but it can be inferred from this result that the main part of narrow signal is due to peptide not bound to membranes. The lowest contribution of narrow signal detected with thylakoids was found to be 16% in buffer at 24 $\mu$M ALA-Aca-CP and 4 mg/ml Chl.

When ethanol (4% saturated the effect) was added to vesicle or thylakoid samples in the absence of CrOx, the narrow signal increased proportional to and usually at the expense of the broad component present (Figs. 6c and d). Addition of unlabelled alamethicin will narrow the lines of labels broadened by interactions in aggregates of a finite size. We checked that this did not work here.

It is of some interest whether the CrOx-inaccessible population of spins is directed to the inner volume of vesicles or only sufficiently shielded, e.g., by charges of lipid head-groups. Tempone was used to estimate the inner aqueous volume of vesicles [59]. Even at very high concentrations of lipid (LUV and SUV, up to 40 mg/ml) at concentrations of 0.5–1 $\mu$M ALA-CP and ALA-Aca-CP, and at about 8 $\mu$M ALA-$Gly_3$-Aca-CP, a slow decrease of the volume occurred, presumably due to a permeabilisation of CrOx. In thylakoids the internal signal of Tempamine [15] was used, which showed a decrease at concentrations as low as about 20 nmol ALA-Aca-CP $mg^{-1}$Chl. Proton transport could be measured with the DTA-method at up to 350 nmol ALA $mg^{-1}$Chl, presumably because part of the DTA in the inner volume is inaccessable to CrOx [15]. When vesicles or chloroplasts were treated with nonpermeabilizing amounts of alamethicin labels (i.e., low concentrations giving a bad signal-to-noise ratio), comparison with samples sonicated in presence of CrOx did reveal only very small changes in shape and height of the spectra, indicating no detectable narrow signal due to alamethicin C-termini in the internal free water space. The same holds when vesicles were prepared with CrOx inside, and regardless of the type of vesicles used.

*Polarity at the C-terminus of alamethicin*

The $A_{zz}$ component of the nitrogen hyperfine splitting can be estimated from rigid glass spectra of samples frozen in liquid nitrogen after reducing a considerable part of the external signal with ascorbate. $A_{zz}$ was approximately equal to the value found in octanol (3.5–3.6 mT, whereas 3.78 mT were found in water at pH 9 and 3.45 in dioxane). This technique may cause some displacement of the label during the freezing of the membrane and the spectra may contain some spins of the population exposed to the outer volume because the half-times of reduction are not sufficiently different from a complete separation (data not shown). Similar information can be obtained from the motion-averaged splitting in room-temperature spectra, which gives only a lower limit of polarity in slowly rotating populations since then the high-field line will be slightly shifted due to incomplete averaging [60]. The splitting (in units of magnetic field strength) obtained from the broad signals in presence of CrOx was very close to the value in water (1.59 vs. 1.62 mT in water, 1.46 mT in dioxane, 1.54 mT in 1-octanol). Heating of samples up to 32°C, i.e., changes in membrane order did not affect this value within experimental precision.

*Signal changes during ion transport*

When thylakoids are illuminated, the ESR spectra become complicated by the presence of a background due to signal I (and to a negligible amount due to signal II) of the photosynthetic electron-transport chain [61,62] and by the reduction of spin-labels by the electron-transport chain [63]. We could reduce the second problem by using FeCy at 1–5 mM, which also serves as Hill-acceptor. Fig. 7 shows the correction procedure which solves the first one: the kinetics taken at the negative midfield peak of the spectra (arrow in Fig. 7c) showed only fast, reversible and slow, irreversible changes (Fig. 7a and b gives the background signal), therefore ESR spectra could be taken in the light (Fig. 7c) and corrected with a background without label (Fig. 7d) using the expected symmetry of the spectra (Fig.

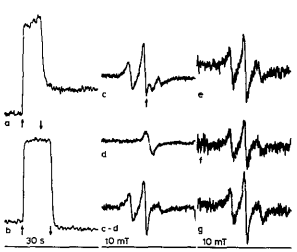


Fig. 7. Changes of ESR spectra of ALA-CP (a, c and d) and ALA-Aca-CP (e–g) and endogenous background (b and d) during electron transport in thylakoids. (a) Kinetics taken on negative midfield peak of a sample (see arrow in (c)). Scan 30 s, shutter hand operated, 20 mW, 83 $\mu$T, $\tau = 100$ ms, 10 scans accumulated, 0.92 mg/ml Chl, 37.5 mM CrOx, 25 mM Tricine, 0.3 M sorbitol, 15 mM KCl, 3.75 mM $MgCl_2$, 2.5 mM FeCy, 5.4 nmol ALA-CP/mg Chl (pH 7.5). (b) As (a), but without label, same field position. (c) Spectra, scan 2 min, $\tau = 0.1$ s, conditions as in (a) and (b), but 0.41 mg/ml Chl, 100 mM Tricine (pH 7.5) and 40 mW microwaves, 18 nmol ALA-CP/mg Chl. (d) As (c) but without label. (e)–(g) Spectra, scan 2 min, $\tau = 0.1$ s, after subtraction of background multiplied by an empirically chosen factor (see text) as in (c) and (d). Conditions as in (e) but 0.58 mg/ml Chl, 10 mW, 53 $\mu$T, 43 nmol/mg Chl ALA-Aca-CP, 33 mM Tricine (pH 7.3). (f) Illuminated. (g) Dark after light.

7c–d). Spectra without CrOx were corrected with the corresponding spectra with CrOx to obtain the effects on the narrow lines only. KCl was used to compensate for changes in ionic strength as far as it was possible without degradation of the samples (see legends). A direct correction of kinetics is not possible since the amount of signal I was found to depend on the prehistory of the sample and particularily on the ion gradients at the membrane [64]. During the measurements the pH of the sample shifts, since electron transport in the presence of FeCy leads to acidification. Figs. 7e, f and g show the effect observed: a marked reversible decrease of the signal in the light. Figs. 8a and b gives the amplitudes of the nitroxide lines under these conditions. Since the lines are passed at different times in spectra, the heights are corrected to the values at the time the midfield peak is passed under the assumption of a constant rate of the irreversible reduction during scans.

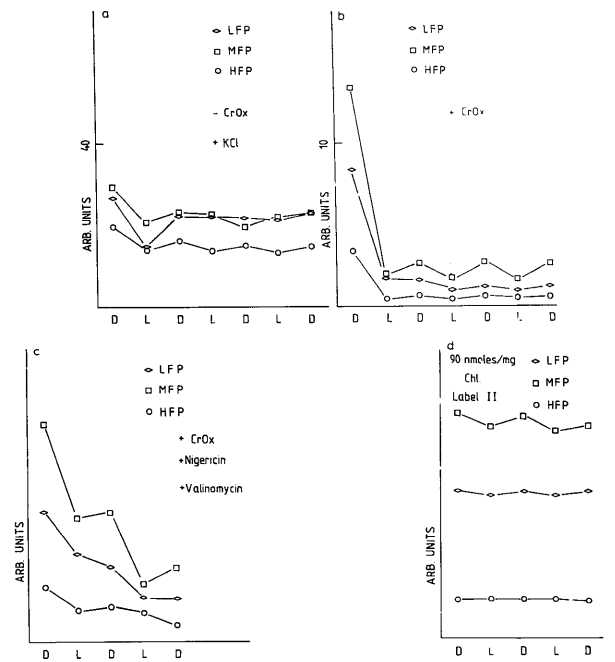


Fig. 8. Height of nitroxide-lines of ALA-Aca-CP in successive scans in light and dark taken from spectra as in Fig. 7e–g, light scans are corrected for irreversible reduction during the scan (to value of midfield line assuming constant rate in the light); HFP, MFP, LFP: heights of high-, middle- and low-field lines. (a) 0.3 M sorbitol, 4.21 mM $MgCl_2$, 126 mM KCl, 2.5 mM FeCy, 33 mM Tris (pH 7.5) to 5.5, 20 mW, 66 $\mu$T, 0.58 mg/ml Chl, 43 nmol ALA-Aca-CP/mg Chl, after subtraction of spectra under identical conditions (see b) but with CrOx, procedure like Fig. 6c–d. (b) as (a) but 17 mM KCl, 40 mM CrOx, after subtraction of spectra without label. The arrow indicates the amount of label undergoing the reversible reaction, see discussion. (c) 0.3 M sorbitol, 0.75 mM $MgCl_2$, 3 mM KCl, 33 mM Tricine (pH 7.2 to 5.5), 40 mM CrOx, 1.6 mM FeCy, 40 mW, 53 $\mu$T, 0.89 mg/ml Chl, 11.1 nmol ALA-Aca-Cp/ml, 55 nmol/mg Chl nigericin, 11.1 nmol/mg Chl valinomycin; subtracted spectra without label. (d) 40 mW, 53 $\mu$T, 0.5 mg/ml Chl, 1.5 mM FeCy, 45 mM Tris (pH 7.5), 5 mM $MgCl_2$, 20 mM KCl, 0.3 M sorbit, 90 nmol/mg Chl ALA-Aca-CP, subtracted spectra without label.

This irreversible reduction of the signal diminishes after several light/dark cycles and the mentioned reversible reduction of the lines can be seen rather undisturbed (Fig. 8b). This effect usually is most pronounced on the midfield line. The reversible reaction is less marked (often even absent) on the narrow (Fig. 8a) than on the broad (Fig. 8b) lines of the spectrum.

FeCy partly suppresses the irreversible reduction, acceleration of the electron transport accentuates it (Fig. 8c). In contrast, the reversible change is essentially unaffected by both conditions.

The herbicide DCMU, blocking electron transport, was found to suppress both effects (this is an internal check of the correction applied, since signal I is higher under these conditions than in a normal sample). Ionophores collapsing ion gradients and potential differences (Fig. 8c) induced only a slight diminution of the reversible effect. When the concentration of label was increased, a smaller fraction of the spectrum turned over in the reversible process (Fig. 8d). Addition of unlabelled alamethicin up to a 60-fold in excess to the labelled species did not abolish the reaction (not shown).

## Discussion

The motion parameters obtained from the spectra refer to motion of the nitroxide itself with but a minor contribution of conformational changes of the peptide. In agreement with this notion the rotations of the immobilized alamethicin labels from vesicles are faster than that of nitroxides attached, e.g., to big helices (compare Ref. 52 or the rotation of the N-terminal label in melittin Ref. 12).

The shape of the broad component is very similar to that reported for spin-labelled melittin in membranes [12]. Our data on polarity point to a position of the label near the membrane surface. While the assignment of broad to bound and narrow to free signal seems obvious, the different amounts of broad, immobilized signal with different derivatives call for an explanation. At present we cannot exclude completely some heterogeneity of the population with narrow signal, i.e., narrow lines from 'bound' peptide but the low amount of this signal with ALA-Aca-CP and high chlorophyll concentrations indicates that this fraction is small ( < 16% of the total signal, and smaller in vesicles).

We are led to postulate a marked difference of the distribution of helices with the structure of the derivatives. This would mean that small changes in the very part of the molecule not entering the membrane were to bring about pronounced changes in its partitioning. This could be understood if we were to assume that the binding is governed by an aggregation which may indeed be changed by small structural variations in the C-terminal part of the helix affecting the stability of aggregates Apparently, this is not the case here (see below), although C-terminal structural variations can influence binding and/or insertion of monomers in membranes.

Although we have seen only slight variations of the signal with CrOx in permeabilized and nonpermeabilized vesicles, our knowledge of the polarity of alamethicin gating strongly suggests there should be a population of spins directed inward [9,10,42]. The quick onset of alamethicin action on the proton gradient seen in fluorescence measurements argues in favour of a quick crossing of the membrane by the peptide. The alternative mechanism to postulate would be back gating, which, however, is improbable with unmodified alamethicin [9]. Our failure to detect narrow signals from the inner volume indicates that there is only bound alamethicin directed inward. Signals of small, freely diffusable labels like Tempamine or Tempone have successfully been employed to measure internal volumes in similar samples (see e.g. Ref. 15).

Aggregates should lead to line broadening by dipolar interaction and Heisenberg exchange which can be reduced by dilution as found with tetrameric melittin in aqueous solution [12] and with solutions in hexane of the compounds studied here. Since the spectra are essentially unaffected by addition of unlabelled alamethicin, we have to conclude that there is a huge excess of monomeres in the membrane or that broadening due to spin-spin interactions in these aggregates is either weak or not easily suppressed by mixing in unlabeled peptide. The finding that the C-terminus of the bound population is located rather deep in the membrane (inaccessibility to CrOx, immobilization) corroborates earlier findings with alamethicin and fluorescence-labelled alamethicin analogues [8,65] and Raman and CD-data [21,66]. It is in agreement with several recent reports [8,10,65] of alamethicin spanning the membrane or crossing it rather easily, a notion supported by the instantaneous action of alamethicin on thylakoids in the light, i.e., in a system with a voltage of the 'wrong' polarity applied, which closely ressembles the situation in the experiments of Schindler [10].

The additional signal in Fig. 4 has not yet found a detailed structural explanation.

The 9AA method used for permeability measurements is in somewhat controversial discussion. Note that only relative values are used here, which are thought to be reliable [67]. Exponents found in the literature for the voltage-independent conductance are 2 to 3 [9,68], a report [69] of up to 7 is believed to be in error. The high exponents found with a method which tends to underestimate them severely indicate voltage-dependent gating. The insensitivity of the exponents found and the spectral changes to the addition of other ionophores does not rule out a voltage-dependence, since the potential in thylakoids is generated initially by the passage of a charge across the membrane on a nanosecond time

scale which is followed by free ions appearing slower (ms). Although the charge is quickly compensated by ion movements [70], this local event may trigger a pore in its vicinity before it is discharged by other ionophores.

Under flashing light, channel formation is clearly demonstrated by the disappearance of the rapid phase of proton deposition (Fig. 3). Voltage-gated channel formation by ALA has been demonstrated in thylakoids [40], using electrochromic absorption changes. We conclude that alamethicin and its derivatives most probably show the same mechanism of voltage-dependent channel formation in our model system as in black lipid bilayer experiments. Upon continuous illumination, a part of the bound population giving rise to the broad spectral lines is affected. The partial disappearance of the signal could be explained by a reversible reduction of the nitroxide [63], which seems improbable since acceleration of electron transport does not accentuate the effect. A more probable hypothesis invokes rearrangements in aggregates giving rise to increased spin-exchange and broadening. Since in hexane dilution with unlabelled alamethicin seems to make broadened signals reappear, whereas the effect in question appears unaffected, we feel inclined to refute this hypothesis as well. The effect is not due to increased accessibility of part of the label to CrOx since it is clearly present in the absence of line-broadening agent.

We conclude that the population giving rise to the broad signals suffers a further hindrance of rotation leading to the reduction of line heights of broad signals) by some change of the arrangement of the peptide in the membrane, whereas there is little or no redistribution between membrane and outer volume (i.e., narrow and broad signal) in the range of concentrations probed. This range covers those concentrations where channel formation occurs as well under continuous as under flashing light in thylakoids (50–300 nmol ALA-derivative $mg^{-1}$Chl depending on the conditions and the derivative used).

The results do not bear upon a postulated helix flip-flop, since we are not able to assign an orientation to the population showing the response.

If one channel is needed to discharge a coupling unit, i.e., a (functionally) closed volume, then 470 molecules of alamethicin turn over in the reversible reaction (at 46 nmol/mg Chl; the quantity measured is indicated by the arrow in Fig. 7b) and still more at higher concentrations of alamethicin rather than the ten expected to form a pore. From a model calculation it follows that a channel conductivity of $2 \cdot 10^{-11}$ S [71] is sufficient to discharge completely a coupling unit. While some caution is advisable in the interpretation of such model calculations, the number found may indicate that we are seeing a change in arrangement (possibly a field effect on peptides in the membrane) out of which only few molecules form a channel in a subsequent step.

Kinetics measured on the time scale of minutes will always show secondary effects superimposed on the primary event. Flash-induced transients should reveal the primary events. Up to now, however, we have not been able to cope with the endogeneous signals obscuring the nitroxide transients.

In summary, we have shown that alamethicin can be spin-labelled without changing its channel-forming properties. Thylakoids can be used as a model system to demonstrate the effects of applied potentials on ionophores. The gating event detected here apparently involves changes in the conformation of membrane bound peptide assembly rather than redistribution of peptide between aqueous solution and membrane.

**Acknowledgements**

B. Wille wishes to thank Professor Dr. H. Ninnemann, who kindly provided the HR9 amplifier, Professor Dr. H. Stegmann for being allowed to use his ESR Spectrometer and data system (financed by the Deutsche Forschungsgemeinschaft), and P. Schuler for expert help with these instruments. B. Wille was a recipient of a doctorate scholarship of the Studienstiftung des Deutschen Volkes. We also acknowledge the support of the Deutsche Forschungsgemeinschaft (SFB 323, project C2-Jung).

**References**

1 Mueller, P. and Rudin, D.O. (1968) Nature 217, 713–719.
2 Latorre, R. and Alvarez, O. (1981) Physiol. Rev. 61, 77–150.
3 Baumann, G. and Mueller, P. (1974) J. Supramol. Struct. 2, 538–557.
4 Boheim, G. and Benz, R. (1978) Biochim. Biophys. Acta 507, 262–270.
5 Boheim, G., Hanke, W. and Jung, G. (1983) Biophys. Struct. Mech. 9, 181–191.
6 Menestrina, G., Voges, K.P., Jung, G. and Boheim, G. (1986) J. Membr. Biol. 93, 111–132.
7 Jung, G., Becker, G., Schmitt, H., Voges, K.P., Boheim, G. and Griesbach, S. (1984) in Peptides. Proceedings 8th American Peptide Symposium (Hruby, V. and Rich, D.H., eds.), pp. 491–494, Pierce Chemical Composition Rockford IL, U.S.A.
8 Voges, K.-P., Jung, G. and Sawyer, W.H. (1987) Biochim. Biophys. Acta 896, 64–76.
9 Hall, J.E., Vodyanoy, I., Balasubramanian, T.M. and Marshall, G.R. (1984) Biophys. J. 45, 233–247.
10 Schindler, H. (1979) FEBS Lett. 104, 157–160.
11 Schwarz, G., Gerke, H., Rizzo, V. and Stankowski, S. (1987) Biophys. J. 52, 685–692.
12 Altenbach, Ch. and Hubbell, W.L. (1988) Proteins 3, 230–242.
13 Bailar, J.C. and Jones, E.M. (1939) Inorg. Synth. 1, 35–38.
14 Rosen, G.M. (1974) J. Med. Chem. 17, 358–360.
15 Wille, B. (1988) Biochim. Biophys. Acta 936, 513–530.
16 Reusser, F. (1968) J. Biol. Chem. 242, 243–247.
17 Balasubramanian, T.M., Kendrick, N.C.E., Taylor, M., Marshall, G.R., Hall, J.E., Vodyanoy, I. and Reusser, F. (1981) J. Am. Chem. Soc. 103, 6127–6132.
18 Katz, E., Schmitt, H., Aydin, M., König, W.A. and Jung, G. (1985) Liebigs Ann. Chem. 365–377.

19 Schmitt, H. and Jung, G. (1985) Liebigs Ann. Chem. 321–344.
20 Brückner, H. and Jung, G. (1980) Chromatographia 13, 170–174.
21 Jung, G., Dubischar, N. and Leibfritz, D. (1975) Eur. J. Biochem. 54, 395–409.
22 Martin, D.R. and Williams, R.J.P. (1976) Biochem. J. 153, 181–190.
23 Irmscher, G. and Jung, (1977) Eur. J. Biochem. 80, 165–174.
24 Brückner, H., König, W.A., Aydin, M. and Jung, G. (1985) Biochim. Biophys. Acta 827, 51–62.
25 Schmitt, H. and Jung, G. (1985) Liebigs Ann. Chem. 345–364.
26 Sane, N., Yoshida, M., Hirata, H. and Kagawa, Y. (1977) J. Biochem. 81, 519–524.
27 Hauska, Y. and Nelson, N. (1986) Methods Enzymol. 126, 285–293.
28 Arnon, D.J. (1949) Plant. Phys. 24, 1–15.
29 Johnsson, S.M., Bangham, A.D. and Korn, E.D. (1971) Biochim. Biophys. Acta 233, 820–826.
30 Reeves, J. and Douwber, R.M. (1969) J. Cell Phys. 3, 47–60.
31 Slovacek, R.E. and Hind, G. (1981) Biochim. Biophys. Acta 635, 393–404.
32 Tilberg, J.E., Giersch, C. and Heber, U. (1977) Biochim. Biophys. Acta 461, 31–47.
33 Haraux, F. and de Kouchkovsky, Y. (1980) Biochim. Biophys. Acta 592, 153–168.
34 Polya, G.M. and Jagendorf, A.T. (1969) Biochim. Biophys. Res. Commun. 36, 696–703.
35 Schönfeld, M. and Schideler, H. (1984) FEBS Lett. 167, 231–234.
36 Schönfeld, M. and Schlott-Kopeliovitch, B. (1985) FEBS Lett. 193, 79–82.
37 Veach, V.R., Mathies, R., Eisenberg, M. and Stryer, L. (1975) J. Mol. Biol. 99, 75–92.
38 Coppinger, C.M. (1957) J. Am. Chem. Soc. 79, 501.
39 Bevington, P.R. (1969) Data Reduction and Error Analysis for the Physical Sciences. McGraw-Hill, New York.
40 Zinkler, A., Witt, H.T. and Boheim, G. (1976) FEBS Lett. 66, 142–148.
41 Tiemann, R. and Witt, H.T. (1982) Biochim. Biophys. Acta 681, 202–211.
42 Junge, W., Ausländer, W., McGreer, A.J. and Runge, T. (1979) Biochim. Biophys. Acta 546, 121–141.
43 Schröder, H., Muhle, R. and Rumberg, B. (1971) Proc. 2nd International Congress on Photosynthesis Research (Forti, G., Avron, M. and Rumberg, B.,eds.), Vol. 2, pp. 919–930, Jung, The Hague.
44 Theg, S.P. and Junge, W. (1983) Biochim. Biophys. Acta 723, 294–307.
45 Polle, A. and Junge, W. (1986) FEBS Lett. 198, 263–267.
46 Keith, A.W., Snipes, W. and Chapman, D. (1977) Biochemistry 16, 634–641.
47 Stone, T.J., Nordio, P.L. and McConnell, H.M. (1965) Proc. Natl. Acad. Sci. USA 57, 1010–1017.
48 Windle, J. (1981) J. Magn. Res. 45, 432–439.
49 Bales, B.L. (1980) J. Magn. Res. 38, 193–205.
50 Bales, B.L. (1982) J. Magn. Res. 48, 418–430.
51 Kusnetsov, A.N., Volkov, A.J., Livshits, V.A., Mirozotian, A.T. and Runge, P. (1974) Chem. Phys. Lett. 26, 369–372.
52 Wee, J. and Millner, J. (1973) J. Phys. Chem. 77, 187–189.
53 Schwarz, G. and Savino, P. (1982) Biophys. J. 39, 211–219.
54 Rizzo, V., Schwarz, G., Voges, K.-P. and Jung, G. (1985) Eur. Biophys. J. 12, 67–73.
55 Schwarz, G., Savko, P. and Jung, G. (1983) Biochim. Biophys. Acta 728, 419–428.
56 Yager, T.D., Eaton, G.R. and Eaton, S.S. (1979) Inorg. Chem. 18, 725–727.
57 Berg, S.P. and Nesbitt, D.M. (1979) Biochim. Biophys. Acta 548, 244–250.
58 Kvielson, D. (1960) J. Chem. Phys. 33, 1094–1106.
59 Vistness, A.J. and Pushkin, J.S. (1981) Biochem. Biophys. Acta 644, 244–250.
60 Griffith, O.H. and Jost, P.C. (1976) in Spin-labelling (Berliner, L.J., ed.), pp. 454–519. Academic Press, New York.
61 Warden, J.T. and Butler, J.R. (1974) Photochem. Photobiol. 20, 251–262.
62 Babcock, G.T. and Sauer, K. (1975) Biochim. Biophys. Acta 376, 329–344.
63 Briggs, S.P., Haug, A.R. and Scheffer, R.P. (1982) Plant Physiol. 70, 662–667.
64 Tikhonov, A.N., Khomuto, G.B., Runge, E.K. and Blumenfeld, L.A. (1981) Biochim. Biophys. Acta 637, 321–333.
65 Vogel, H., Nilsson, L., Rigler, R., Voges, K.-P. and Jung, G. (1988) Proc. Natl. Acad. Sci. USA 85, 5067–5071.
66 Vogel, H. (1987) Biochemistry 26, 4562–4574.
67 DeBenedetti, E. Garlaschi, F.M. (1977) J. Bioeng. Biomembr. 9, 195–201.
68 Roy, G. (1975) J. Membr. Biol. 24, 71–85.
69 Cherry, R.J., Chapman, D., Graham, D.E. and Shaper, J.H. (1977) Ann NY Acad. Sci. 303, 281–291.
70 Junge, W. (1977) Annu. Rev. Plant. Phys. 28, 503–536.
71 Sakmann, B. and Boheim, G. (1979) Nature 282, 336–339.